Nuclear Engineering and Design 291 (2015) 287–294

Contents lists available at ScienceDirect

Nuclear Engineering and Design

journal homepage: www.elsevier.com/locate/nucengdes

Safety verification of radiation shielding and heat transfer for a dry spent fuel storage model

Haiyan Yu[a,b], Xiaobin Tang[a,b,*], Peng Wang[a,b], Feida Chen[a,b], Hao Chai[a,b], Da Chen[a,b]

[a] Department of Nuclear Science and Engineering, Nanjing University of Aeronautics and Astronautics, Nanjing 210016, China
[b] Jiangsu Key Laboratory of Nuclear Energy Equipment Materials Engineering, Nanjing 210016, China

HIGHLIGHTS

- New type of dry spent fuel storage was designed.
- MC method and FEM were used to verify the reliability of new storage.
- Radiation shield and heat transfer both meet IAEA standards: 2 mSv/h, 0.1 mSv/h and 190 °C, 85 °C.
- Provided possibilities for future implementation of this type of dry storage.

ARTICLE INFO

Article history:
Received 18 November 2014
Received in revised form 5 May 2015
Accepted 17 May 2015

Classification:
S. Waste management

ABSTRACT

The goal of this research is to develop a type of dry spent fuel storage called CHN-24 container, which could contain an equivalent load of 45 GWD/MTU of spent fuel after 10 years cooling. Basically, radiation shielding performance and safe removal of decay heat, which play important roles in the safety performance, were checked and validated using the Monte Carlo method and finite element analysis to establish the radiation dose rate calculation model and three-dimensional heat transfer model for the CHN-24 container. The dose rates at the surface of the container and at a distance of 1 m from the surface were 0.42 mSv/h and 0.06 mSv/h, respectively. These conform to the International Atomic Energy Agency (IAEA) radioactive material transportation safety standards 2 mSv/h and 0.1 mSv/h. The results shows that the CHN-24 container maintains its structural and material integrity under the condition of normal thermal steady-state heat transfer as well as in case of extreme fire as evinced by transient-state analysis. The temperature inside and on the surface of the container were 150.91 °C and 80 °C under normal storage conditions, which indicated that the design also conform to IAEA heat transfer safety standards of 190 °C and 85 °C.

1. Introduction

Nuclear safety is always stressed as the top priority when developing a nuclear power facility. At present, the nuclear industry is rapidly developing in China. Ensuring the safety of nuclear spent fuel storage and its transportation are important parts of this endeavour. However, as the world's nuclear powers are gradually extending their use of dry storage for spent fuel (Saegusa et al., 2010), there is neither enough dry storage for nuclear spent fuel with independent intellectual property in China, nor sufficient related research into dry spent fuel storage.

Therefore, in this work, in view of the fact that nuclear power stations are producing increasing amounts of spent fuel of burn-up rating 45 GWD/MTU in China, and that there are insufficient dry storages meeting this supply. The preliminary work before designing a type of dedicated container (CHN-24) for spent fuel, which can store 24 groups of spent fuel assemblies, proceed with referring to the dry containers which have superior performance (Chikazawa et al., 2009), meanwhile, in consideration of the actual production and manufacturing technology available for nuclear spent fuel dry storage containers. In this paper, associated safety evaluations of container are discussed, which accord to the regulations for the safe transport of radioactive material (International Atomic Energy Agency (IAEA) Safety Standards Series No. 6 TS-R-1199

* Corresponding author at: Department of Nuclear Science and Engineering, Nanjing University of Aeronautics and Astronautics, 29 Yu dao St., Nanjing 210016, China. Tel.: +86 13601582233.
E-mail addresses: yuhaiyan@nuaa.edu.cn (H. Yu), tangxiaobin@nuaa.edu.cn (X. Tang), wp739130046@nuaa.edu.cn (P. Wang), fdchen@nuaa.edu.cn (F. Chen), chaihao@nuaa.edu.cn (H. Chai), chenda@nuaa.edu.cn (D. Chen).

http://dx.doi.org/10.1016/j.nucengdes.2015.05.021
0029-5493/

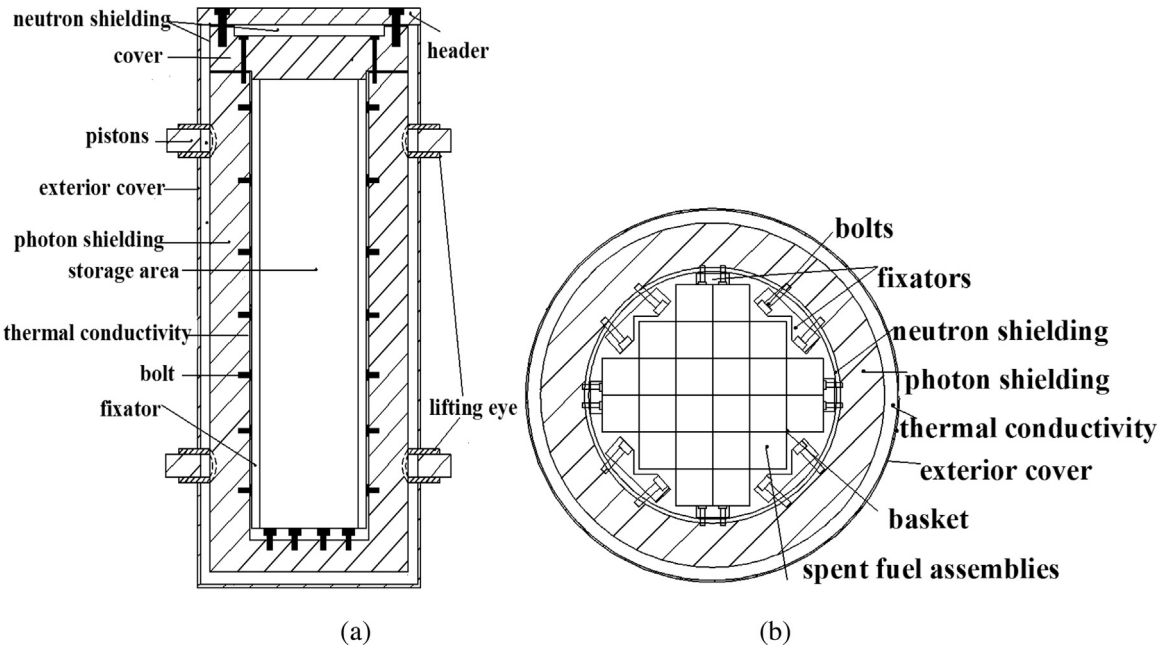

Fig. 1. Diagram of CHN-24 container structures: (a) longitudinal section and (b) transverse section.

Edition (2003) As Amended, IDT). Actually, the CHN-24 container is designed along with studying its radiation shielding performance (Iqbal et al., 2006) and heat transfer characteristics (Santo Domingo et al., 1998) using Monte Carlo method and finite element analysis (Hammersley and Handscomb, 1964).

2. Models and methods

Due to some unsafe effects arising from spent fuel which include its continual radioactivity and decay heat generation, the new CHN-24 container must be designed to meet IAEA Safety Standards Series No. TS-R-1: the safe upper limit of dose at the surface of the container which has contained spent fuel is 2 mSv/h, and at a distance of 1 m from the container falls to 0.1 mSv/h; the whole container could use natural air circulation for cooling when spent fuel is stored. Therefore, the following study has been carried out for this CHN-24 container to validate its safety performance: (1) dose calculation and (2) heat transfer analysis.

2.1. Details of CHN-24 container model

The CHN-24 container designed here was cylindrical with a total height of container of 440 cm, the maximum height of spent fuel assemblies of 370 cm, and its inner diameter measuring 152 cm. In order to improve the thermal performance of the whole container, copper was chosen to constitute the photon shield (Keech et al., 2014). Due to cost effectiveness, Type 304 stainless steel was selected as main photon shield material, which has good photon shielding effectiveness and a high melting point by around 200 °C. PPC-H.O.T.-NSC resin matrix composite material was used as neutron shield material, due to it has a relatively high melting point by around 176 °C with good neutron shield performance.

The photon shield on the curved side of the container with a total thickness of 32 cm (externally mounted), and a thickness of 31 cm on both ends, which consists of a copper layer (thickness of 3 cm on the curved side, and 10 cm on both ends) and a Type 304 stainless steel layer (thickness of 29 cm on the curved side, and 21 cm on both ends). Outside the photon shielding layer, lay the 6 cm thickness of a neutron shielding layer which made of PPC-H.O.T.-NSC resin matrix composite materials (manufactured in USA). Then, 1 cm thickness of Type 304 stainless steel as cladding formed the outermost layer. There are eight blocks measuring 4 cm × 20 cm × 270 cm evenly disposed around the hanging basket holder for spent fuel assemblies within (Fig. 1).

2.2. Dose calculations

Spent fuel, retired from nuclear reactors, is radioactive and emits photons and neutrons. If there is a lack of radiation shielding to its containers, the environment and humans will be damaged. MCNP code is used widely in nuclear technology including dose calculation for designing neutron shields to nuclear reactors, accelerators, and radioactive environments. MCNP is well-known for precise radiation dosimetry according to ICRP validation. MCNP5 was therefore used here in the dose calculation for this container and its 24 groups of spent fuel assemblies.

According to the materials chosen for the CHN-24 dedicated container model, a dose calculation model container was established along with 24 groups of 17 × 17 spent fuel assemblies (Hammersley and Handscomb, 1964). The length and height of each fuel assembly are 270 cm and 23.61 cm, respectively which includes the fuel rods whose diameter is 1.33 cm, the thickness of the hanging basket for spent fuel is an additional 1 cm.

The MCNP repeated structures cards: U cards (described only once, can be designated to fill each of any number of cells in the geometry) and FILL cards were utilized to improve the reliability and speed of dose calculations, we refined the internal structures of the spent fuel assembly model by using MCNP multi-level U and FILL cards, which means the cells in a universe themselves are filled with another universes. There is a maximum of 10 levels, here, 4 levels U-FILL cards were used to construct the dose calculation model. As a result, all of the fuel rods, neutron measuring tubes, and absorbing rods which make up each group of spent fuel assemblies were established respectively: a total of 6936 of these units were used (Fig. 2).

The burn-up level of spent fuel assemblies, with initial fuel enrichment of 4.0 wt% ^{35}U, is 45 GWD/MTU (after ten years cooling), and the constituents of the spent fuel obtained from the book

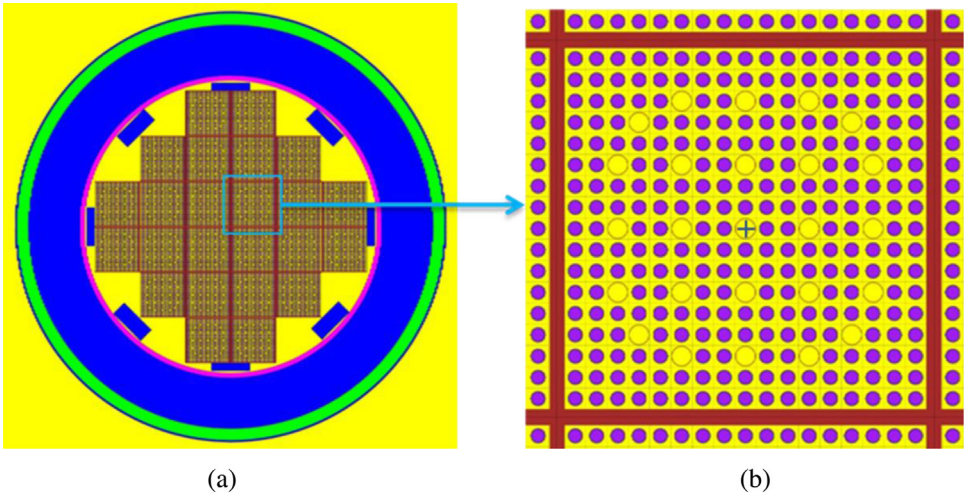

Fig. 2. CHN-24 container model in MCNP: (a) cross-section and (b) details of one fuel assembly, which consists of: fuel rods (red circles), absorbing rods (yellow circles), neutron measurement tube (circle with a plus sign). (For interpretation of the references to colour in this figure legend, the reader is referred to the web version of this article.)

(Broadhead et al., 1995.). The neutron and photon energy spectrums for each spent fuel assembly are shown in Fig. 3. MCNP source cards: SI and SP cards were used to describe the source terms (shown in Fig. 3) in MCNP input files. A total of 24 groups of spent fuel assemblies were simulated as a whole source term on condition that each fuel assembly was considered as a separate source. Dose contributed by neutrons and photons was calculated using the MCNP tally f6 (energy deposition tally, MeV/g), and tally FM6 was adopted which values were respectively set as 5.48812E13 (for photons) and 5.916672E6 (for neutrons) to convert energy deposition to dose rate (mSv/h).

The equivalent symmetric method was used to study the dose rate of the CHN-24 container. Considering that the whole container is symmetrical, simulations were carried out to calculate the dose rate of the container, which ranged from the central shaft to the edge of one side and from the central plane to upper surface, to represent the dose rate values radially and axially of the whole container. In consideration of the influence of the spent fuel storage containers on the surrounding environment, doses induced by neutrons and photons at different distances from the container surface were calculated separately.

2.3. Heat transfer analysis

Finite element analysis, which solves the problem by dividing the solution domain into many interconnected finite domains, then each subdomain assumes a suitable approximate solution to derive boundary constraints, the right solution will be got till entire subdomains are satisfied. It is used widely to solve practical problems, especially in case of complicated geometry and physical field.

Here, finite element software COMSOL was employed, which contains a large number of predefined physics application patterns, including solid heat transfer and radiation heat transfer as well as other physical fields. It supports multiple physical field coupling and can simulate heat transfer in spent fuel containers while providing accurate temperature fields in and around the container. According to the materials and construction of CHN-24 container, a dedicated physical field model-based simulation was set-up. For the complex structures in these CHN-24 containers, it was difficult to establish this model if the native modelling functions of COMSOL was used. So pre-processing with SOLIDWORKS bridged this gap to the COMSOL software and simplified the process of modelling the heat transfer effectively. Heat transfer simulation was based on the

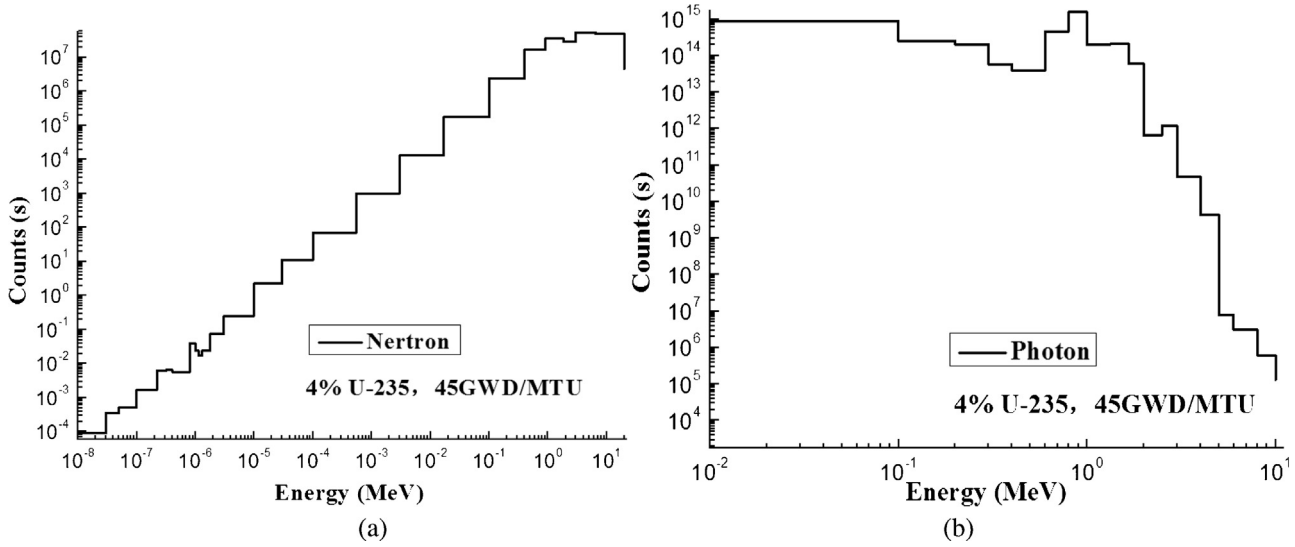

Fig. 3. Source terms of 45 GWD/MTU fuel assemblies: (a) neutron energy spectrum and (b) photon energy spectrum.

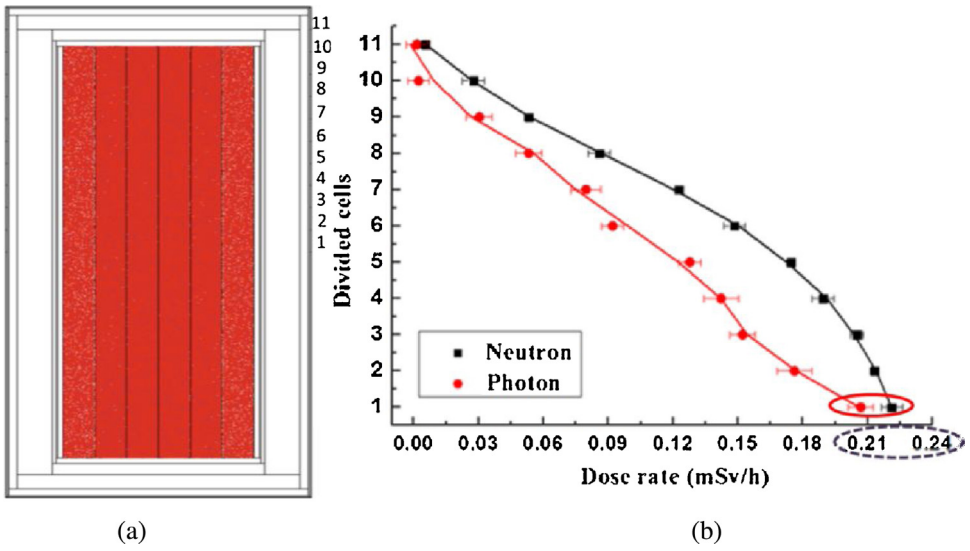

Fig. 4. Dose calculation model for CHN-24: (a) cells divided on the surface and (b) radial distribution of dose rate.

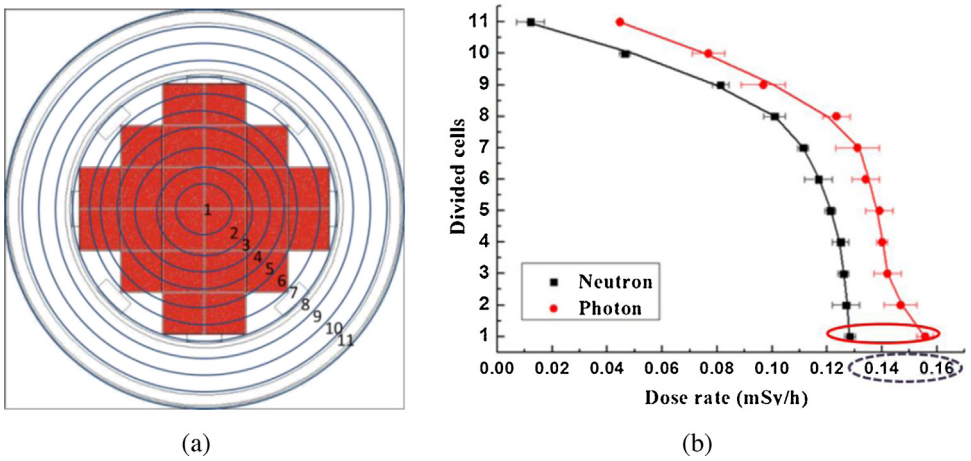

Fig. 5. Dose on the surface of the CHN-24 container: (a) cross-section of source terms and (b) axial distribution of dose rate.

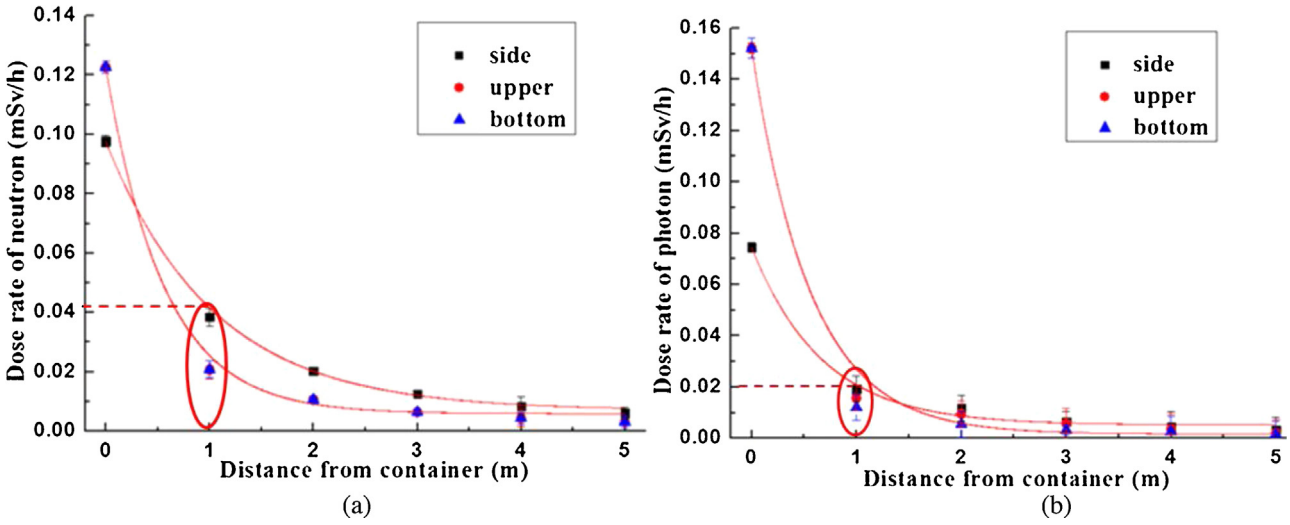

Fig. 6. Dose distribution around the container: (a) neutron dose and (b) photon dose.

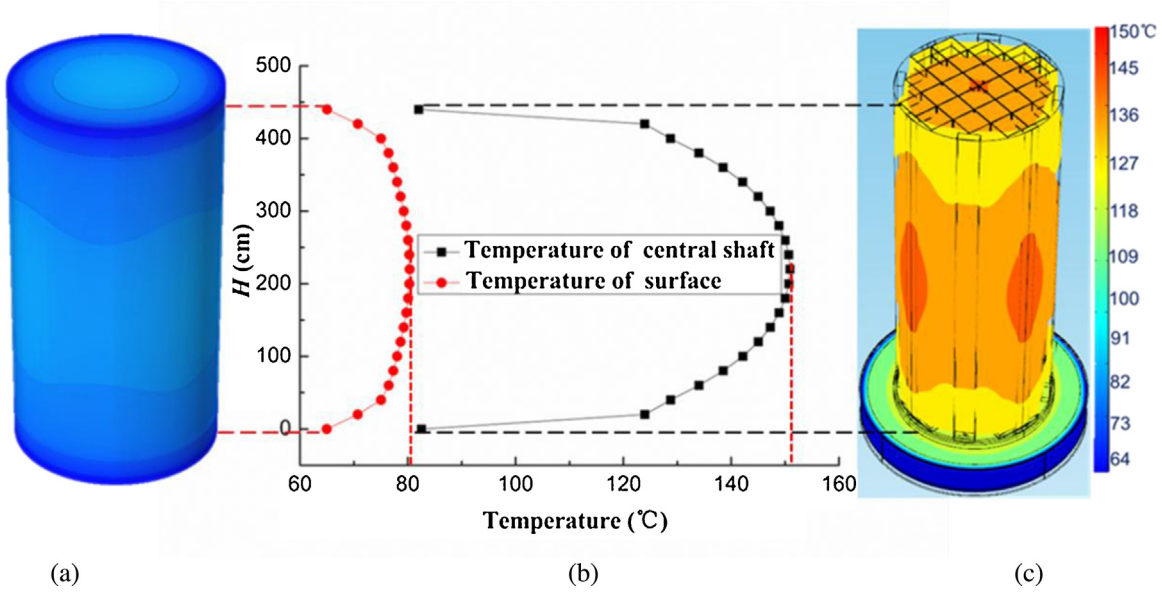

Fig. 7. Temperatures of CHN-24 container: (a) surface temperature, (b) curves of temperatures at different heights and (c) inside temperature of container.

solid heat transfer coupled radiation heat transfer physical fields by solving the heat conduction equation for a homogeneous air system using the Newton iterative solutions. Each element uses a different equation based on the results generated from the surrounding elements. The equation used to approximate conduction through a solid is given in the following equation:

$$\rho C_p u_{\text{trans}} \nabla T = \nabla \times (k \nabla T) + Q \quad (1)$$

where ρ = material density; C_p = specific heat; u_{trans} = translational motion vector; ∇T = temperature gradient; k = thermal conductivity; Q = heat generation.

The change in temperature depends on the thermal conductivity (k) and the heat generation (Q) of each fuel rod. The initial temperature was set to 293.15 K, each of the fuel rods has calorific power of 2.44 W (Iqbal et al., 2006) on condition that the spent fuel, after being retired from the reactor, had been cooled for ten years. Here, 264 fuel rods were contained in each group of spent fuel assemblies, so the heating power of all of the spent fuel components inside the container was about 15.5 kW.

Additionally, air-driven natural convective cooling was adopted to represent the model of the surrounds to the container (Roychowdhury et al., 2002). The key to finite element modelling lies in the meshing calculation. Due to the complexity of such container structures, discontinuous in mesh boundaries arise, meanwhile, it is essential to choose a suitable grid size in order to ensure the reliability of the heat transfer simulation results. So a tetrahedral grid domain division was applied for the container, and for the sake of accuracy, the boundary grid was refined.

Two solution steps were conducted in each specific heat transfer calculation to verify heat transfer compliance with IAEA safety standards. The steady-state analysis was used to calculate the temperature field under normal storage conditions. Then the container

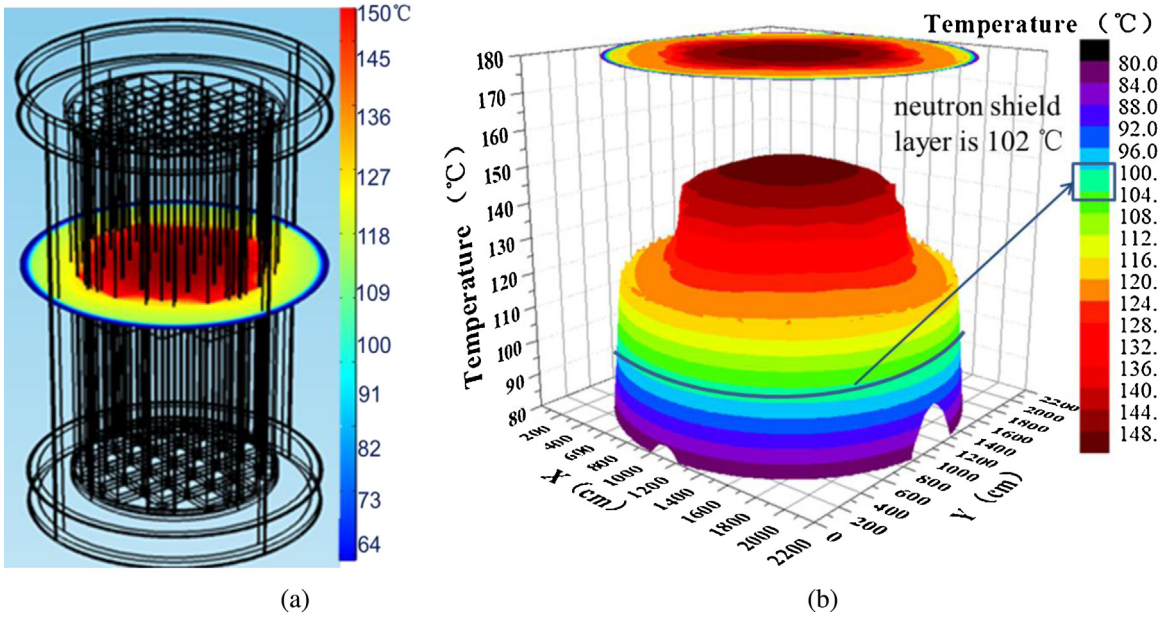

Fig. 8. Temperature distribution of transverse section at the middle height in CHN-24 container: (a) diagram in COMSOL and (b) plotting in ORIGIN.

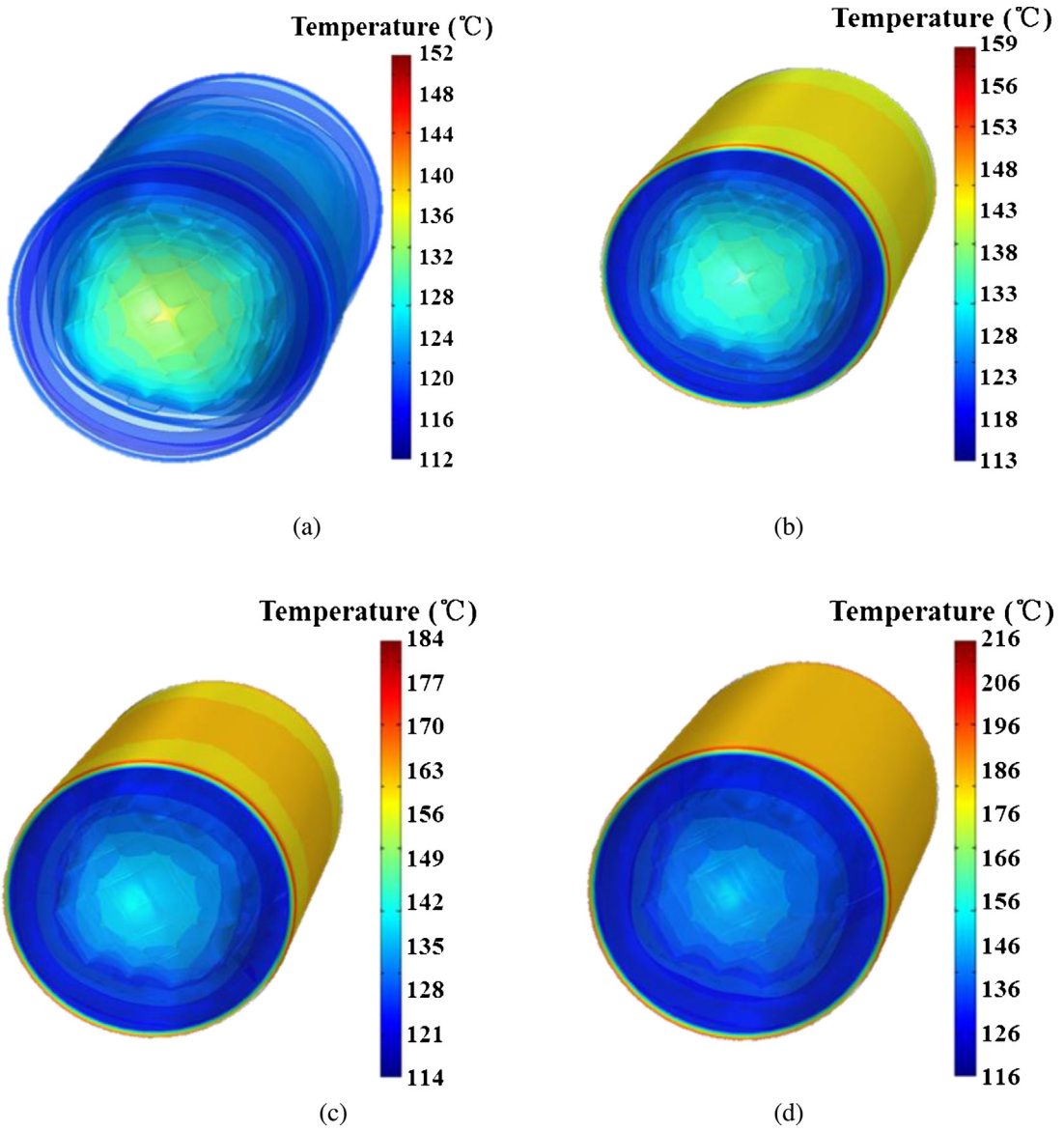

Fig. 9. Temperature changes over time in accident of fire: (a) 10 min, (b) 20 min, and (c) 30 min, (d) 40 min after fire happened.

temperature change over time in the event of an extreme fire was assessed by transient analysis, paying special attention to structural and material integrity, and in particular to assess whether it remained undamaged or not after 30 min.

3. Results and discussion

3.1. Radiation dose at the container surface

The sectional drawings of the CHN-24 container model in the MCNP visualisation are shown in Figs. 4a and 5a. In addition, In order to calculate the dose rate to surface of container, 1 cm thickness of cylinder with two bottoms, consists of tissue equivalent material, was as the exterior cladding to the CHN-24 container. And it was divided into 11 separate cells in the axial and radial directions.

The error bars represent the Monte Carlo statistical uncertainty of dose rate calculation for CHN-24 container and the error ratios are all less than 2%, which meet the accuracy of calculation by Monte Carlo method.

The dose distribution curve to the surface of the CHN-24 container is shown in Figs. 4b and 5b, dose rates to radial and axial surfaces both gradually decreased from the centre of symmetry to the edge. The changes in dose induced by photons and neutrons irradiance in an axial direction was similar, yet changes of dose rate induced by neutrons in the radial direction was relatively flat as demonstrated by the transition rate, in that dose induced by neutrons being slower than that induced by photons decreased from the centre to the edge of the container (Chen et al., 2013). As seen in Figs. 4b and 5b, on the surface of container, the peak dose induced by neutrons and photons was 0.42 mSv/h: this was within the IAEA's upper limit of 2 mSv/h.

3.2. Radiation dose to the container's surrounds

The dose at different distances (0 m to 5 m) from the ends and sides was calculated (see Fig. 6). Dose induced by photons and neutrons decreased exponentially with distance from the CHN-24 container. In the distance of 1 m from surface of container, the peak dose induced by neutrons and photons was 0.06 mSv/h: this was lower than the IAEA's upper limit of 0.1 mSv/h.

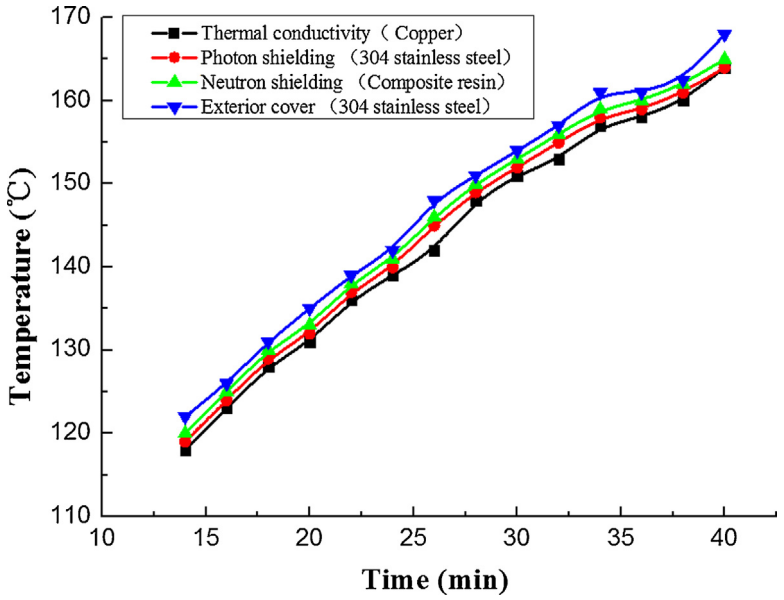

Fig. 10. Temperature variations of shielding layers with time in accident of fire.

3.3. Temperature of the container under normal conditions

The maximum and minimum temperature of each *X*–*Y* cross-section every 20 cm from $H = 0$ cm to $H = 440$ cm (*i.e.* from bottom to top) is shown in Fig. 7.

Fig. 7 shows that both maximum and minimum temperatures decreased from the centre to edge, and the maximum temperature inside the container underwent a greater change than the minimum on the container surface.

The highest temperature inside the CHN-24 container was 150.91 °C which was lower than the IAEA upper limit of 190 °C, and much lower than the 300 °C maximum temperature that materials inside the container could withstand. The highest temperature on the surface of the CHN-24 container was 80 °C, also lower than the IAEA upper limit of 85 °C.

From the analysis of above, the maximum temperature inside the container decreased from middle to edge, so the temperature distribution along a cross-section at mid-height ($H = 220$ cm) of the container could be used to characterize the highest temperature anywhere in the container. In order to assess the heat transfer safety of the container, observing the temperatures in the neutron shielding layer, which has the poorest heat resistance, and assessing whether it was below its melting point or not.

Fig. 8 shows the across-section at mid-height, the temperature gradually decreased from the centre outwards (the 24 groups of spent fuel assemblies were deemed to be a decay heat source). According to Fig. 8b, the temperature of the neutron shielding material was 102 °C, far below its 176 °C melting point. Therefore it could be concluded that CHN-24 containers can retain their structural integrity and that of their constituent materials in good condition using natural air circulation for cooling.

3.4. Temperature of the container under extreme fire conditions

Heat transfer simulation of CHN-24 container was carried out using COMSOL software: when the external extreme fire occurred, it was assumed that the ambient temperature rose to 800 °C. Then a study of the temporal and spatial temperature variations was undertaken by transient analysis.

Fig. 9 shows that temperature distributions of container at four moments, respectively 10 min, 20 min, and 30 min, 40 min since the fire occurred. It can be seen that the temperature became higher as time went on. The temperature of container surface was the highest, and in the centre of container was the second high. While, the temperatures of photon and neutron shield layers were lower than both above-mentioned.

Fig. 10 shows that the temperature of each layer in the container wall increased with the on-going duration of the fire. The difference in temperature across each shielding layer was 1 °C, of which the outer cladding was the hottest, and also changed the fastest. Compared with other materials in each layer, the heat-resisting performance of the neutron shielding material was the worst especially when considering its temperature change over time. As fire lasts for 30 min, the temperature of the neutron shielding layer rose to 153 °C, however which still below its melting point of 176 °C. However, within 30 min since the fire occurred, the CHN-24 container maintained its structural and material integrity and met the IAEA safety standards for heat transfer.

4. Conclusions

The safety performance of the CHN-24 container was verified: the container was designed independently for storing 24 groups of spent fuel assemblies with burn-up level of 45 GWD/MTU after 10 years cooling.

The dose rates at the surface of the container and at a distance of 1 m are 0.42 mSv/h and 0.06 mSv/h, which conform to the prescribed IAEA standards for radioactive material transportation. The dose rate decreases exponentially from the centre to the edge of the container as well as along the distance from the surface of the container to farther.

Under normal storage conditions, the temperature inside and on the surface of the container are 150.91 °C and 80 °C, respectively: these meet the IAEA regulations for safe temperature operations. In the event of an extreme fire accident, the CHN-24 container retains its structural and material integrity for 30 min: this also conforms to IAEA safety standards.

This study verified safety aspects such as those pertaining to safe enclosure of radioactive materials and safe removal of decay heat for the CHN-24 dedicated container. This provided possibilities for future implementation of this type of dry spent fuel storage.

Acknowledgements

This work was supported by the Project supported by the Specialized Research Fund for the Doctoral Program of Higher Education of China (Grant No. 20123218120028), Project supported by the Foundation of Graduate Innovation Center in NUAA (Grant No. kfjj20150602), Project supported by the Cooperative innovation fund project of Jiangsu Province (Grant No. BY2014003-04) and Project supported by the Funding of Jiangsu Innovation Program for Graduate Education (Grant No. KYLX0266).

References

Broadhead, B.L., DeHart, M.D., et al., 1995. Investigation of Nuclide Importance to Functional Requirements Related to Transport and Long-Term Storage of LWR Spent Fuel. J. ORNL/TM-12742. Lockheed Martin Energy Systems, Inc., Oak Ridge National Laboratory.

Chikazawa, Y., et al., 2009. Technology gap analysis on sodium-cooled reactor fuel-handling system supporting advanced burner reactor development. J. Nucl. Technol. 165 (3), 270–292.

Chen, Y.F., et al., 2013. Effects of source and geometry modeling on the shielding calculations for a spent nuclear fuel dry storage cask. J. Nucl. Technol. 182 (2), 224–234.

Hammersley, J.M., Handscomb, D.C., 1964. Monte Carlo Methods. Methuen, M. London.

Iqbal, M., Khan, J., Mirza, S.M., 2006. Design study of a modular dry storage facility for typical PWR spent fuel. J. Prog. Nucl. Energy 48 (6), 487–494.

Keech, P.G., Ramamurthy, S., et al., 2014. Design and development of copper coatings for long term storage of used nuclear fuel. J. Corros. Eng. Sci. Technol. 49 (6), 425–430.

Roychowdhury, D.G., Das, S.K., Sundararajan, T., 2002. Numerical simulation of natural convective heat transfer and fluid flow around a heated cylinder inside an enclosure. J. Heat Mass Transfer. 38 (7), 565–576.

Santo Domingo, J.W., et al., 1998. Microbiology of spent nuclear fuel storage basins. J. Curr. Microbiol. 37 (6), 387–394.

Saegusa, T., et al., 2010. Review and future issues on spent nuclear fuel storage. J. Nucl. Eng. Technol. 42, 237–248.

Further reading (bibliography listing)

Journals

Cracknell, R.F., Gordon, P., Gubbins, K.E., 1993. Influence of pore geometry on the design of microporous materials for methane storage. J. Phys. Chem. 97 (2), 494–499.

DeHart, M.D., 1996. Sensitivity and Parametric Evaluations of Significant Aspects of Burnup Credit for PWR Spent Fuel Packages. Oak Ridge National Lab. TN (United States). Funding Organisation: USDOE, Washington, DC.

Fukuda, K., Danker, W., Lee, J.S., Bonne, A., Crijns, M.J., 2003. IAEA overview of global spent fuel storage. In: Proceedings of an International Conference on Storage of Spent Fuel from Power Reactors, June, 2003, IAEA in cooperation with OECD/NEA, Vienna, pp. 2–6.

Hopf, J.E., 1995. Conceptual design report for the DUCRETE^{TM} spent fuel storage cask system. INEL 95, 0030.

Ilas, G., Rahnema, F., 2003. A Monte Carlo based nodal diffusion model for criticality analysis of spent fuel storage lattices. J. Ann. Nucl. Energy 30 (10), 1089–1108.

Lee, Y.S., Kim, H.S., Kang, Y.H., Chung, S.H., Choi, Y.J., 2004. Effect of irradiation on the impact and seismic response of a spent fuel storage and transport cask. Nucl. Eng. Des. 232 (2), 123–129.

Patrick, W.C., 1986. Spent Fuel Test-Climax: An Evaluation of the Technical Feasibility of Geologic Storage of Spent Nuclear Fuel in Granite: Final Report. Lawrence Livermore National Lab, CA (USA).

Pearce, K.L., 1998. 105-K Basin Material Design Basis Feed Description for Spent Nuclear Fuel Project Facilities. Volume 2: Sludge (No. HNF-SD-SNF-TI–009-Rev. 2). Fluor Daniel Hanford Inc., Richland, WA.

Wu, Z., Lin, D., Zhong, D., 2002. The design features of the HTR-10. J. Nucl. Eng. Des. 218 (1), 25–32.

Patents

Bevilacqua, F., 1977. U.S. Patent No. 4,024,406. Washington, DC: U.S. Patent and Trademark Office.

Congleton, R.L., Flynn, W.M., Henry, C.W., & Machado, O.J., 1993. U.S. Patent No. 5,245,641. Washington, DC: U.S. Patent and Trademark Office.

Daugherty, D.A., Flanders Jr, H.E., Georges, N.J., & Machado, O.J., 1988. U.S. Patent No. 4,781,883. Washington, DC: U.S. Patent and Trademark Office.

Books

Niederreiter, Harald, 1992. Random Number Generation and Quasi-Monte Carlo Methods, vol. 63. Society for Industrial and Applied Mathematics, Philadelphia (Books).

Zienkiewicz, Olgierd Cecil, Morice, P.B., 1971. The Finite Element Method in Engineering Science, vol. 1977. McGraw-hill, London.

Banerjee, Prasanta Kumar, Roy, Butterfield, 1981. Boundary Element Methods in Engineering Science, vol. 17. McGraw-Hill, London.

Website or Webpage

Kintisch, Eli, March, 2011. Contention over Risk of Fire from Spent Fuel Pools.
Backgrounder on Dry Cask Storage of Spent Nuclear Fuel. September 22, 2014.
Dry Cask Storage. July 07, 2014.